Desalination and Water Treatment
www.deswater.com
doi: 10.5004/dwt.2020.26499

207 (2020) 115–121
December

Preparation and characterization of TiO_2 modified with APTMS for phenol decomposition

Agnieszka Wanag*, Paulina Sienkiewicz, Ewelina Kusiak-Nejman, Antoni W. Morawski

Faculty of Chemical Technology and Engineering, Department of Inorganic Chemical Technology and Environment Engineering, West Pomeranian University of Technology in Szczecin, Pułaskiego 10, 70-322 Szczecin, Poland, emails: awanag@zut.edu.pl (A. Wanag), paulina.sienkiewicz@zut.edu.pl (P. Sienkiewicz), Ewelina.Kusiak@zut.edu.pl (E. Kusiak-Nejman), Antoni.Morawski@zut.edu.pl (A.W. Morawski)

Received 11 February 2020; Accepted 20 August 2020

ABSTRACT

In this work, physicochemical and photocatalytic properties of titanium dioxide nanomaterial modified with 3-aminopropyltrimethoxysilane (APTMS) is presented. The photocatalyst was obtained by a two-step solvothermal and calcination method at 700°C in an argon atmosphere. The tested materials were characterized by means of X-ray diffraction, scanning electron microscopy, Fourier-transform infrared spectroscopy/diffuse reflectance spectroscopy (UV-Vis/DRS). The Brunauer–Emmett–Teller specific surface area as well as pore size distribution were also measured. It was noted that the APTMS modification played a significant role in phase transformation changes, crystallite size as well as values of the specific surface area. It was found that the transformation from anatase to rutile was suppressing after APTMS modification. The photocatalytic activity of the obtained samples was determined by the phenol photodegradation under artificial solar light. The photocatalyst after aminosilanes modification and calcination exhibited higher photoactivity than TiO_2-starting and the sample obtained similarly but without the addition of APTMS.

Keywords: Photocatalysis; TiO_2; 3-aminopropyltrimethoxysilane (APTMS); Phenol photodecomposition; Artificial solar light

1. Introduction

In recent years, the best known and examined photocatalyst seems to be titanium dioxide (TiO_2). Despite many advantages like high stability, low cost of production or safety toward humans and the environment, it has important disadvantages as follows: low absorption of visible radiation or rapid recombination of electron-hole pairs [1]. Furthermore, the physicochemical properties of TiO_2 such as particle size, pore-volume, surface area and crystallinity also play a crucial role in photoactivity. Notably, a high crystallinity is one of the most critical factors that determine a high photoactivity [2]. However, in order to achieve a good crystallinity of the photocatalyst, the high-temperature treatment is necessary. On the other hand, with the increasing calcination temperature the crystallite size and rutile amount in the sample increase whereas the specific surface area decreases [3,4]. It is widely known that the photocatalytic efficiency is higher when physiochemical parameters are optimal. In the literature can find that the optimal particle size of anatase crystallite for the best photoactivity is around 10 nm [5]. The surface area should be large due to a large amount of adsorbed organic pollutants promotes the photocatalytic process [6,7]. It is also well-known that anatase is generally considered as the more efficient photocatalyst than rutile and brookite [8,9]. Thus TiO_2 should be modified in a way as to obtain a sample with high crystallinity while maintaining other optimal physicochemical

* Corresponding author.

parameters. It has been reported that Si has the property of phase transformation inhibitor [10]. For this purpose, some modifications were carried out [11–15]. One of the compounds containing silicon atoms in the structure are aminosilanes, such as 3-aminopropyltrimethoxysilane (APTMS) [16,17], 3-aminopropyltriethoxysilane (APTES) [18,19] or the most commonly known tetraethyl orthosilicate [18,20]. There are only a few reports on enhancing the photocatalytic activity of different hybrid APTMS-TiO_2 nanomaterials. Photong and Boonamnuayvitaya [16] prepared SiO_2–TiO_2 photocatalytic films by the condensation of methyltrimethoxysilane and APTMS dedicated to the improvement of indoor air quality. They obtained a film with a 15 times larger surface area than the unfunctionalized one. It was found that the APTMS-functional group influenced the specific surface area. Khantamat et al. [17] synthesized anatase titanium dioxide particles functionalized by APTMS with the addition of partial gold shells destined for removing the methylene blue. It was found that the APTMS-TiO_2 functionalized material was characterized by higher stability, which had prevented aggregation of the prepared photocatalyst.

Information about the influence of TiO_2 modification with APTMS, especially on the physicochemical properties of TiO_2 after calcination is limited in the literature. In this work, we report the preparation of TiO_2/Si nanomaterials obtained from TiO_2 provided by chemical plant Grupa Azoty Zakłady Chemiczne "Police" S.A. (Poland) and APTMS as a new Si precursor. The preparation process consists of a two-step solvothermal and calcination method at 700°C in an argon atmosphere. Our fundamental motivation for using APTMS was not the only improvement of TiO_2 physiochemical properties but also improvement photoactivity by the presence of nitrogen and carbon from APTMS.

2. Experimental setup

2.1. Preparation

TiO_2 supplied by sulfate technology from Chemical Plant Grupa Azoty Zakłady Chemiczne "Police" S.A. (Poland) was used as a starting material. Due to the content of 2.1 wt.% of residual sulfur (from post-production sulphuric acid) in TiO_2 material, the crude titanium dioxide has been pre-treated to reach pH 6.8 before modification. For this purpose, the crude titanium dioxide was rinsed with a solution of ammonia water (25% solution, Avantor Performance Materials, LLC, Poland S.A.) and then some time with distilled water. When the solution reached pH 6.8, TiO_2 was dried at 105°C for 24 h in a muffle furnace. The final material was denoted as TiO_2-starting. The new photocatalyst was obtained in two steps. Firstly, 5 g of TiO_2-starting and 50 mL of APTMS (97% Merck KGaA, Germany) solutions with a concentration of 5.6 mM in ethanol (98%, Firma Chempur, Poland) were mixed and transferred to a pressure autoclave BR-100 (Berghof Products + Instruments GmbH, Germany). The sample was heated at 100°C with continuous stirring for 12 h. The obtained suspension was centrifuged and dried at 100°C overnight. Next, the obtained material was calcined at 700°C for 4 h in Ar atmosphere (60 mL/min, 99.999%, Air Liquide Polska, Poland). The final product was denoted as TiO_2-APTMS-700. The reference sample was obtained based on the same method but without APTMS (denoted as TiO_2-700).

2.2. Characterization

The phase composition and crystal structure were analyzed using X-ray powder diffraction analysis (PANalytical Empyrean X-ray diffractometer, USA) with Cu-Kα radiation (λ = 1.54056 Å). The X-ray diffraction (XRD) diffractograms were collected in the range 10°–80° of 2θ scale. The average anatase crystallite diameter was calculated according to Scherrer's equation Eq. (1) [21].

$$D = \frac{K\lambda}{\beta\cos\theta} \tag{1}$$

where D is the mean crystallite size (nm), λ is the wavelength of Cu Kα radiation (nm), θ is the Bragg's angle (°), β is the calibrated width of a diffraction peak at half maximum intensity (rad).

The anatase and rutile content was calculated according to a simple peak intensity-based method. For these calculations, the most intensive peaks for anatase at 25.4° and rutile at 27.5° were chosen. The percentage of, that is, anatase (%A) was calculated as shown in Eq. (2):

$$\%A = \frac{I_A}{I_A + I_R} \times 100\% \tag{2}$$

where I_A is the intensity of anatase peak at 25.4°, I_R is the intensity of rutile peak at 27.5°.

The 4200 Fourier-transform infrared spectroscopy (FTIR/DRS) spectrophotometer (JASCO International Co., Ltd., Japan) equipped with DiffusIR accessory (PIKE Technologies, USA) was used to study the chemical changes and structural properties of TiO_2 after modification. The UV-Vis diffuse reflectance spectra of the tested materials were recorded on a V-650 spectrophotometer (JASCO International Co. Japan) equipped with a PIV-756 integrating sphere accessory for studying DR spectra (JASCO International Co., Japan). Spectralon (Spectralon® Diffuse Reflectance Material) was used as the standard sample. The Brunauer–Emmett–Teller specific surface area (S_{BET}) was carried out based on adsorption–desorption measurements at 77 K conducted by Quadrasorb SI analyzer (Anton Paar GmbH, Austria, previously Quantachrome Instruments, USA). In order to remove residual water adsorbed and organic carbon residues from the surface of the samples, prior to analysis, all samples were dried and then degassed at 100°C for 24 h, under a high vacuum. The morphology of nanomaterials particles was observed employing scanning electron microscopy utilizing the SU8020 ultra-high resolution field emission scanning electron microscope (Hitachi, Ltd., Japan).

2.3. Photocatalytic test

The photocatalytic activity was investigated by the decomposition of phenol in aqueous solution under artificial solar light in an air atmosphere. In a typical process, 0.1 g of the photocatalyst was added into 500 mL of an aqueous

solution of phenol with an initial concentration of 10 mg/L. The suspension was stirred in darkness for half an hour to reach the adsorption equilibrium between the photocatalyst surface and phenol molecules and then it was illuminated. As an artificial solar light source, a halogen lamp with a radiation intensity of about 0.3 W/m^2 of UV and 720 W/m^2 of Vis was used. After 5 h of irradiation, a 5 mL suspension was taken and centrifuged to separate the TiO_2 nanoparticles from the phenol solution. The phenol concentration was determined utilizing the high-performance liquid chromatography HPLC (Elite LaChrome chromatograph, Hitachi, Ltd., Japan) equipped with a UV detector.

3. Results and discussion

3.1. FTIR/DRS analysis

The FTIR/DR spectra of TiO_2-starting, TiO_2-700 and TiO_2-APTMS-700 photocatalysts are presented in Fig. 1. Some characteristic bands for TiO_2 are observed for all tasted photocatalysts. Broadband located in the range of 3,700–2,600 cm^{-1} is characteristic of stretching vibrations of the absorbed water [22]. The weak band at 3,675 cm^{-1} observed for TiO_2-700 and TiO_2-APTMS-700 samples are assigned to the stretching mode of different types of free hydroxyl groups and it is related to the use of alcohol in the preparation step [23]. The narrowband at 1,640 cm^{-1} is attributed to the stretching and bending modes characteristic of physisorbed water [24]. A characteristic strong peak in the range of 1,000–600 cm^{-1} is assigned to the surface vibrations of the Ti–O bonds [25]. The strong band corresponds to the vibration of the Ti–O–Ti and Ti–O bonds in TiO_2 are located at 960 and 907 cm^{-1}, respectively [26]. The FTIR/DRS analysis confirms the appearance of new bonds after APTMS modification. The low-intensity peak located at 940 cm^{-1} is characteristic of the stretch vibration band of Ti–O–Si [27,28]. Additionally, the peak located around 1,077–1,207 cm^{-1} is attributed to the Si–O–Si bond stretching modes of silanol group corresponding to the condensation reaction between silanol groups [29].

3.2. X-ray diffraction and scanning electron microscopy images analysis

The XRD patterns of tested photocatalysts are shown in Fig. 2. The phase composition and crystallite size of all studied photocatalysts are also listed in Table 1. Based on the results it can be observed that TiO_2-APTMS-700 and TiO_2-starting samples consist mainly of anatase phase (indexed by A, JCPDS 01-070-7348) with a small amount of rutile (ca. 2%, indexed by R, JCPDS 01-076-0318). A reflection of rutile in TiO_2-starting is observed due to the addition of rutile nuclei during the TiO_2 production process (sulfate technology). Thus, the presence of rutile in TiO_2-starting material is not caused by the transformation of anatase to rutile. It is commonly known that the typical TiO_2 phase transformation starts at ~600°C [30]. In this case, the anatase-to-rutile phase transformation is observed for the TiO_2-700 photocatalyst. This sample consists of 86% of anatase and 14% of rutile. What is interesting, the transformation of anatase into rutile was delayed for the TiO_2-APTMS-700 sample. This sample contains only 2% of rutile, while a control TiO_2-700 sample without APTMS modification contains 14% of rutile. It is caused by Si presence in the sample which is a phase transformation inhibitor [10]. It can also be noted that the APTMS modification suppresses crystallites growth from 55 nm for TiO_2-700 to 14 nm for TiO_2-APTMS-700, which was also confirmed by Bao et al. [12] and Klarysri et al. [31]. The morphology of APTMS modification was also confirmed in scanning electron microscopy images. In Fig. 3 it can be observed images of TiO_2-starting, TiO_2-700 and TiO_2-APTMS-700 photocatalysts. The materials consist of not regular and undefined shape particles which aggregated to a larger form. After modification, the decrease of agglomerates size is not observed. The

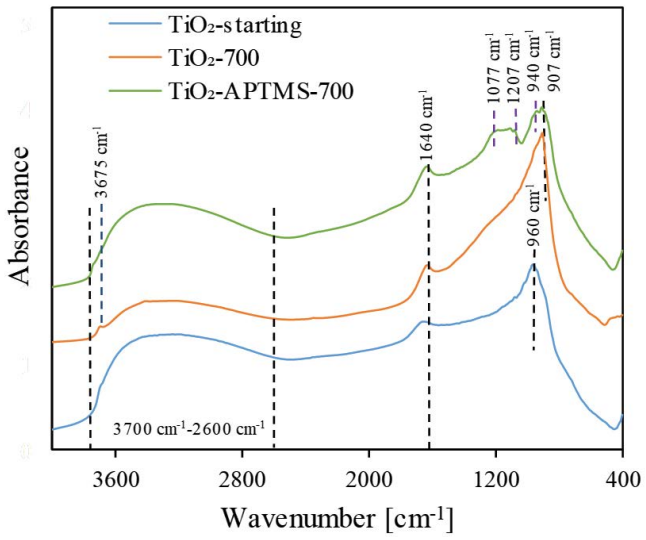

Fig. 1. FT-IR/DR spectra of reference TiO_2-starting, control TiO_2-700 and APTMS-modified TiO_2.

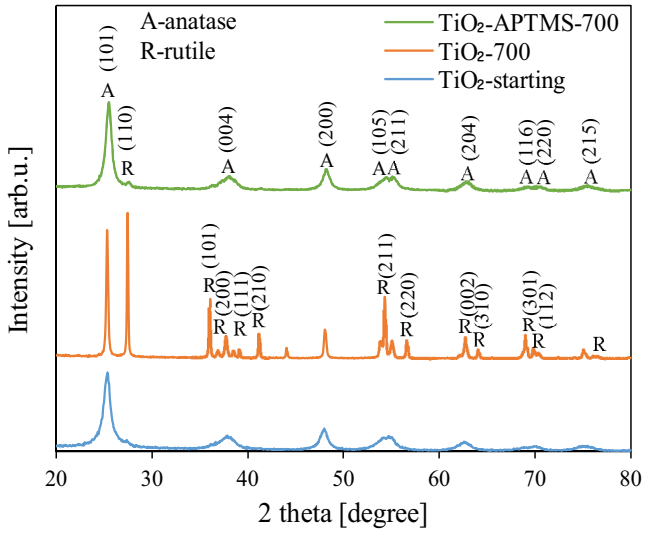

Fig. 2. XRD patterns of reference TiO_2-starting, control TiO_2-700 and APTMS-modified TiO_2.

Table 1
Physicochemical properties of studied photocatalysts

Name sample	Anatase content (%)	Anatase crystallite size (nm)	Rutile crystallite size (nm)	S_{BET} (m^2/g)	V_{total} [a] (cm^3/g)	V_{micro} [b] (cm^3/g)	V_{meso} [c] (cm^3/g)
TiO_2-starting	98	12	15	242	0.34	0.09	0.25
TiO_2-700	86	55	146	16	0.12	0.01	0.11
TiO_2-APTMS-700	98	14	25	170	0.28	0.06	0.22

[a]Total pore volume determined by the signal point nitrogen adsorption isotherms at relative pressures p/p_0 = 0.989.
[b]Micropore volume estimated using the method DR (Dubinin–Radushkevich).
[c]Mesopore volume was determined from the difference V_{total} 0.989 and V_{micro} DR.

photocatalysts were also analyzed by energy-dispersive X-ray analysis (EDX) and shown in Fig. 3d–g. Based on the diagram in Fig. 3d noted the TiO_2-APTMS-700 sample consists of titanium, oxygen and silicon. According to mapping, a uniform distribution of all elements is observed. The silicon content in photocatalyst was equal to ~2 wt.%.

3.3. UV-vis diffuse reflectance analysis

The UV-vis absorption spectra of materials and the spectra are shown in Fig. 4. As can be seen, modification with APTMS did not cause any significant changes in absorption properties. The slight absorption abilities in the visible region are related to color change after the modification process from white for TiO_2-starting to light ECRU for TiO_2-APTMS-700. A similar property is observed for the TiO_2-700 sample thus it can be concluded that color change is correlated to heat treatment at 700°C, not to APTMS modification. A significant redshift in the absorption edge is observed only for TiO_2-700 photocatalyst and it is corresponding to energy band-gap values. The band-gap energy for this sample is 3.2 eV (the band-gap energy for starting-TiO_2 and TiO_2-APTMS-700 is 2.28 eV). In this case, the band-gap narrowing is attributed to changes in the TiO_2 phase composition especially with the presence of rutile in tested samples [32]. Taking into account that modification with APTMS caused suppression of phase transformation, for the TiO_2-APTMS-700 sample containing only 2% of rutile any changes in the band-gap energy are not noted.

3.4. BET analysis

The APTMS modification had not only a great influence on the crystallite size and crystal structures but also on the S_{BET} area of the TiO_2. The BET surface area (S_{BET}) and pore volume (V_m) for the tested photocatalysts are shown in Table 2. Additionally, the N_2 adsorption-desorption isotherms curves of these samples are displayed in Fig. 5. It is widely known that with the increase of calcination temperature, the decrease of the S_{BET} area occurs, which was

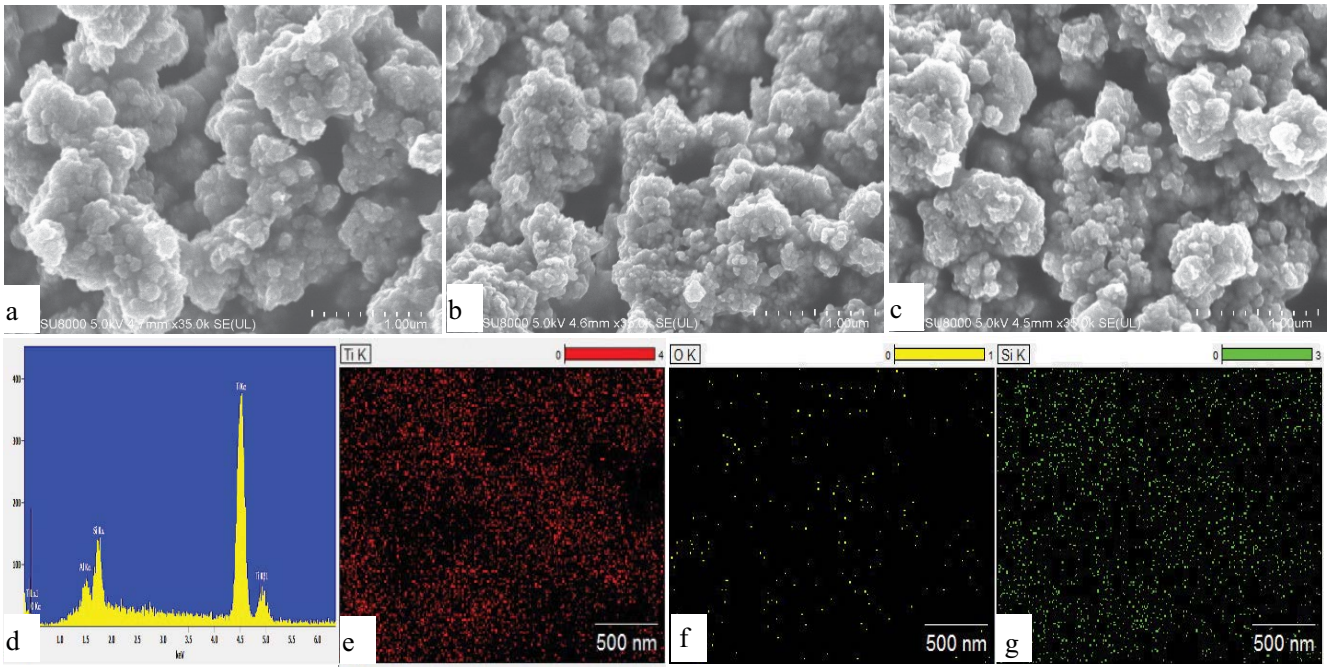

Fig. 3. Scanning electron microscopy image of (a) TiO_2-starting, (b) TiO_2-700, (c) TiO_2-APTMS-700 and (d–g) photocatalysts and EDX spectrum and EDX mappings of TiO_2-APTMS-700.

also observed in the presented study. The temperature of calcination caused a significant decrease in the S_{BET} area from 242 m^2/g for TiO_2-starting to 15 m^2/g for TiO_2-700 and it is a typical process for high temperature [33]. First of all, the effect of the sintering of crystallites occurs [34], and secondly, 14% rutile with large crystallite size was found [35]. Additionally, the S_{BET} area calculated for TiO_2-APTMS-700 photocatalyst equals about 170 m^2/g (Table 1), and it is linked to crystallites growth suppression by Si crystallites growth. After temperature modification at 700°C, it can also be observed a significant reduction of pore size volume of the TiO_2-700 sample. It is worth mentioning that sample after APTMS modification is characterized by two times higher a total pore volume than the TiO_2-700 sample. From Fig. 5, it can be seen that isotherms of all tested nanomaterials present a type IV isotherm, according to the International Union of Pure and Applied Chemistry classification [36]. However, the isotherms of TiO_2-starting and TiO_2-APTMS-700 photocatalysts are very similar and have a bit higher N_2 adsorbed volume than TiO_2-700 nanomaterials what is related to mesoporous structure. These samples exhibit obvious H3 type hysteresis loops, while the TiO_2-700 material displays limited H4 type hysteresis loops. No significant changes in pore structures are mainly attributed to Si modification.

3.5. Photocatalytic activity

The photocatalytic activity of the TiO_2-APTMS-700 photocatalyst in comparison with the TiO_2-starting and TiO_2-700 nanomaterials measured on the basis of the phenol decomposition under artificial solar light is presented in Fig. 6. It should be added that the photolysis test of phenol degradation (without photocatalyst) was negligible. The TiO_2-APTMS-700 nanomaterial demonstrates the highest photoactivity with a degradation degree of 34.15%. In contrast, 10.13% and 14.63% of degradation degree were achieved for TiO_2-starting and TiO_2-700, respectively. The relatively high photoactivity at high-temperature modification is due to several properties: crystallite size, crystal structure and specific surface area. It can be observed that the physicochemical properties of the TiO_2-APTMS-700 sample are similar for TiO_2-starting, which consists mainly of anatase with small crystallite size. Zhang et al. [5] found that the optimal anatase crystallite size for higher photoactivity is about 10 nm. It is also known that the anatase phase is a more active form than rutile [37]. The S_{BET} area value is also an important factor for heterogeneous photocatalysis. It is commonly known that the number of active places depends on the specific surface size. Thus, a photocatalyst with a higher specific surface area is characterized by more number of active sites and is able to adsorb the larger amount of pollutant particles which can be degradation during the photocatalytic process. Taking into account, a photocatalyst after APTMS modification shows higher efficiency than TiO_2-700. Furthermore, the APTMS modification like Ti–O–Si causes not only high thermal stability but also promotes higher photoactivity. Klarysri et al. [31] suggested that higher photoactivity after organosilane modification is related to an increase of the oxygen chemisorption on the TiO_2 surface. The possible mechanism for photocatalytic phenol degradation via modified

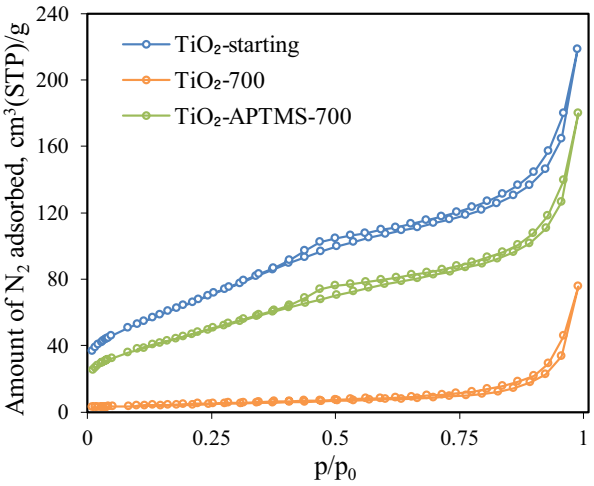

Fig. 5. N_2 adsorption–desorption isotherms for TiO_2-starting, control TiO_2-700 and APTMS-modified TiO_2.

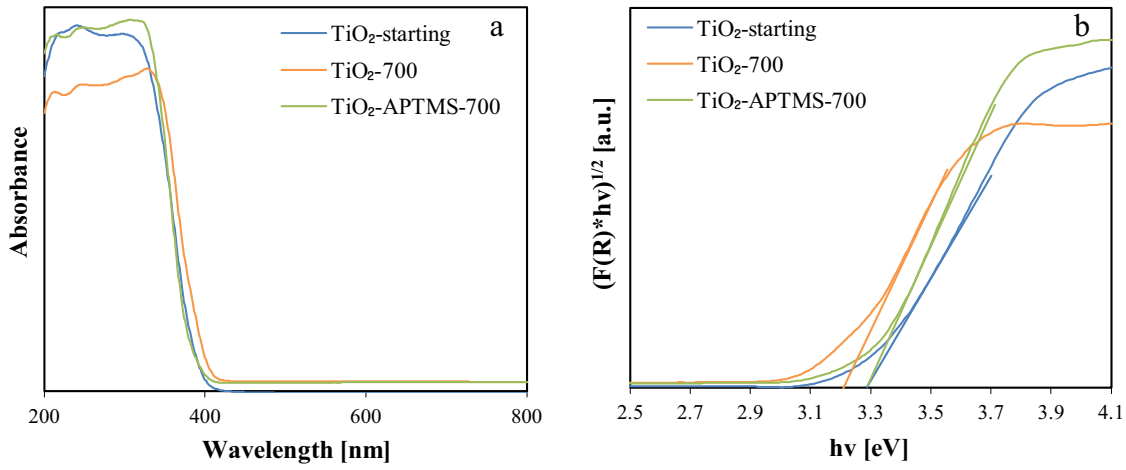

Fig. 4. (a) UV-Vis/DR spectra and (b) Tauc plot of reference TiO_2-starting, control TiO_2-700 and APTMS-modified TiO_2.

nanocomposite is proposed in Fig. 7. During irradiation of the photocatalysts with artificial solar light, electrons from the valance band migrate to the conduction band. Generated electron-hole pairs react with dissolved oxygen species and water molecules forming superoxide joins. The suppression of electron-hole recombination was found as the main role of silicon in the Si-modified TiO_2 photocatalytic process. Su et al. [38] attributed this phenomenon to the increase of the rate of electron diffusion caused by the enhancement of the anatase crystallinity and decrease of bulk defects as the effect of the employment of high-temperature calcination. Thus, the enhanced photoactivity of TiO_2-APTMS-700 is related to the both physicochemical properties of the sample after APTMS modification such as smaller crystallite size, higher anatase content and surface area as well as suppression of recombination rate.

4. Conclusions

In this work, the effect of the APTMS modification on the physicochemical properties of TiO_2, as well as the photoactivity was studied. The presents of APTES were confirmed based on the FTIR/DRS analysis. It was found that the APTMS modification suppressed the phase transformation, the stability of the anatase phase and crystal stability. Consequently, the decrease of the S_{BET} area and total pore volume were inhibited. The photoactivity of the tested nanomaterials was studied by phenol degradation under artificial solar light. The sample after the APTMS modification and calcination at 700°C showed the highest efficiency. The thermal stability of photocatalysts and the presence of Ti–O–Si, which promotes higher photoactivity, play an essential role.

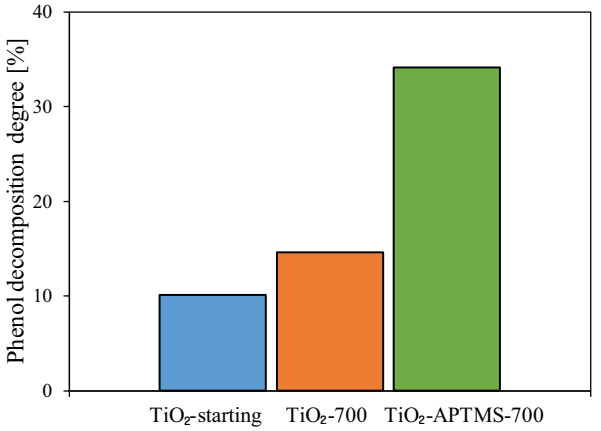

Fig. 6. Phenol decomposition degrees after 5 h irradiation under artificial solar light irradiation.

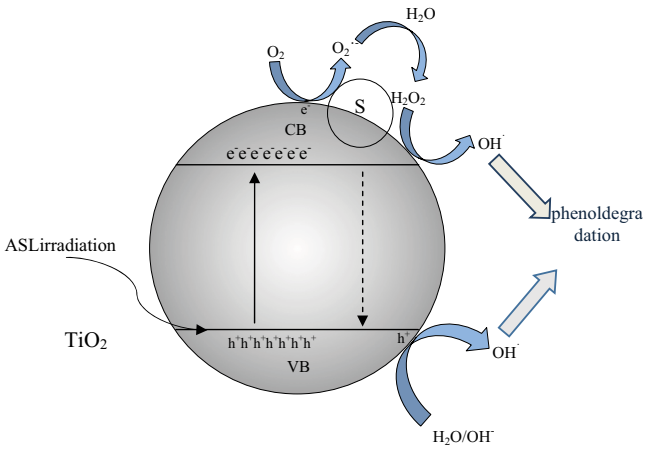

Fig. 7. Scheme of photocatalytic degradation of phenol.

Acknowledgment

This work was supported by grant 2017/27/B/ST8/02007 from the National Science Centre, Poland.

Author contributions

Conceptualization, A.W.; Investigation, A.W., P.S.; Data Curation, A.W. and E.K.-N.; Writing – Original Draft Preparation, A.W.; Writing – Review & Editing, E.K.-N. and A.W.M.; Supervision, A.W.M. All authors read and approved the final manuscript.

References

[1] S.M. Gupta, I.M. Tripath, A review of TiO_2 nanoparticles, Chin. Sci. Bull., 56 (2011) 1639–1657.
[2] S.J. Tsai, S. Cheng, Effect of TiO_2 crystalline structure in photocatalytic degradation of phenolic contaminants, Catal. Today, 33 (1997) 227–237.
[3] J.F. Porter, Y.G. Li, C.K. Chan, Effect of calcination on the microstructural characteristics and photoreactivity of Degussa P-25 TiO_2, J. Mater. Sci., 34 (1999) 1523–1531.
[4] P. Górska, A. Zaleska, E. Kowalska, T. Klimczuk, J.W. Sobczak, E. Skwarek, W. Janusz, J. Hupka, TiO_2 photoactivity in vis and UV light: the influence of calcination temperature and surface properties, Appl. Catal., B, 84 (2008) 440–447.
[5] Z.B. Zhang, C.-C. Wang, R. Zakaria, J.Y. Ying, Role of particle size in nanocrystalline TiO_2-based photocatalysts, J. Phys. Chem. B, 102 (1998) 10871–10878.
[6] D.W. Bahnemann, S.N. Kholiskaya, R. Dillert, A.I. Kulak, A.I. Kokorin, Photodestruction of dichloroacetic acid catalyzed by nano-sized TiO_2 particles, Appl. Catal., B, 36 (2002) 161–169.
[7] Y.X. Chen, K. Wang, L.P. Lou, Photodegradation of dye pollutants on silica gel supported TiO_2 particles under visible light irradiation, J. Photochem. Photobiol., A, 163 (2004) 281–287.
[8] L. Liu, H. Zhao, J.M. Andino, Y. Li, Photocatalytic CO_2 reduction with H_2O on TiO_2 nanocrystals: comparison of anatase, rutile and brookite polymorphs and exploration of surface chemistry, ACS Catal., 2 (2012) 1817–1828.
[9] J.M. Hermann, Heterogeneous photocatalysis: fundamentals and applications to the removal of various types of aqueous pollutants, Catal. Today, 53 (1999) 115–129.
[10] D.A.H. Hanaor, C.C. Sorrell, Review of the anatase to rutile phase transformation, J. Mater. Sci., 46 (2011) 855–874.
[11] P. Cheng, M.P. Zheng, Y.P. Jin, Q. Huang, M.Y. Gu, Preparation and characterization of silica-doped titania photocatalyst through sol–gel method, Mater. Lett., 57 (2003) 2989–2994.
[12] N. Bao, Z.T. Wei, Z.H. Ma, F. Liu, G.B. Yin, Si-doped mesoporous TiO_2 continuous fibers: preparation by centrifugal spinning and photocatalytic properties, J. Hazard. Mater., 174 (2010) 129–136.
[13] A. Mahyar, M.A Behnajady, N. Modirshahla, Characterization and photocatalytic activity of SiO_2–TiO_2 mixed oxide nanoparticles prepared by sol–gel method, Ind. J. Chem., 49A (2010) 1593–1600.

[14] C. Su, K.F. Lin, Y.H. Lin, B.H. You, Preparation and characterization of high-surface-area titanium dioxide by sol–gel process, J. Porous Mater., 13 (2006) 251–258.
[15] A. Nilchi, S.J. Darzi, A.R. Mahjoub, S.R. Garmarodi, New TiO_2/SiO_2 nanocomposites-phase transformations and photocatalytic studies, Colloids Surf., A, 361 (2010) 25–30.
[16] S. Photong, V. Boonamnuayvitaya, Preparation and characterization of amine-functionalized SiO_2/TiO_2 films for formaldehyde degradation, Appl. Surf. Sci., 255 (2009) 9311–9315.
[17] O. Khantamat, C.H. Li, S.P. Liu, T. Liu, H.J. Lee, O. Zenasni, T.C. Lee, C. Cai, T.R. Lee, Broadening the photoresponsive activity of anatase titanium dioxide particles via decoration with partial gold shells, J. Colloid Interface Sci., 513 (2018) 715–725.
[18] N. Bao, G.L. Wu, J.J. Niu, Q.Z. Zhang, S. He, J. Wang, Wide spectral response and enhanced photocatalytic activity of TiO_2 continuous fibers modified with aminosilane coupling agents, J. Alloys Compd., 599 (2014) 40–48.
[19] R. Klaysri, T. Tubchareon, P. Praserthdam, One-step synthesis of amine-functionalized TiO_2 surface for photocatalytic decolorization under visible light irradiation, J. Ind. Eng. Chem., 45 (2017) 229–236.
[20] X. Zhang, F. Zhang, K.-Y. Chan, Synthesis of titania–silica mixed oxide mesoporous materials, characterization and photocatalytic properties, Appl. Catal., A, 284 (2005)193–198.
[21] G. Colón, J.M. Sánchez-España, J.M. Hidalgo, J.A. Novío, Effect of TiO_2 acidic pre-treatment on the photocatalytic properties for phenol degradation, J. Photochem. Photobiol., A, 179 (2007) 20–27.
[22] M. Winter, D. Hamal, X. Yang, H. Kwen, D. Jones, S. Rajagopalan, K.J. Klabunde, Defining reactivity of solid sorbents: what is the most appropriate metric?, Chem. Mater., 21 (2009) 2367–2374.
[23] M. Janus, B. Tryba, M. Inagaki, A.W. Morawski, New preparation of carbon-TiO_2 photocatalysts by carbonization of *n*-hexane deposited on TiO_2, Appl. Catal., B, 52 (2004) 61–67.
[24] X. Chen, D.-H. Kuo, D. Lu, N-doped mesoporous TiO_2 nanoparticles synthesized by using biological renewable nanocrystalline cellulose as template for the degradation of pollutants under visible and sun light, Chem. Eng. J., 295 (2016) 192–200.
[25] H. Auoub, M. Kassir, M. Raad, H. Bazzi, A. Hijazi, Effect of dye structure on the photodegradation kinetic using TiO_2 nanoparticles, J. Mater. Sci. Chem. Eng., 5 (2017) 31–45.
[26] T. Bezrodna, T. Gavrilko, G. Puchkovska, V. Shimanovska, J. Baran, M. Marchewka, Spectroscopic study of TiO_2 (rutile)–benzophenone heterogeneous systems, J. Mol. Struct., 614 (2002) 315–324.
[27] V. Zelenek, V. Hornebecq, S. Mornet, O. Schaf, P. Llewellyn, Mesoporous silica modified with titania: structure and thermal stability, Chem. Mater., 18 (2006) 3184–3191.
[28] E. Ukaji, T. Furusawa, M. Sato, N. Suzuki, The effect of surface modification with silane coupling agent on suppressing the photo-catalytic activity of fine TiO_2 particles as inorganic UV filter, Appl. Surf. Sci., 254 (2007) 563–569.
[29] M.Y. Wan, W.F. Li, Y.M. Long, Y.F. Tu, Electrochemical determination of tryptophan based on Si-doped nano-TiO_2 modified glassy carbon electrode, Anal. Methods, 4 (2012) 2860–2865.
[30] Y. Hu, H.-L. Tsai, C.-L. Huang, Effect of brookite phase on the anatase–rutile transition in titania nanoparticles, J. Eur. Ceram. Soc., 23 (2003) 691–696.
[31] R. Klarysri, S. Wichaidit, T. Tubchareon, S. Nokjan, S. Piticharoenphun, O. Mekasuwandumrong, P. Praserthdam, Impact of calcination atmospheres on the physiochemical and photocatalytic properties of nanocrystalline TiO_2 and Si-doped TiO_2, Ceram. Int., 41 (2015) 11409–11417.
[32] D. Reyes-Coronado, G. Rodriguez-Gattorno, M.E. Espinosa-Pesqueira, C. Cab, R. de Coss, G. Oskam, Phase-pure TiO_2 nanoparticles: anatase, brookite and rutile, Nanotechnology, 19 (2008) 145605–145615.
[33] A.M. Luis, M.C. Neves, M.H. Mendonca, O.C. Monteiro, Influence of calcination parameters on the TiO_2 photocatalytic properties, Mater. Chem. Phys., 125 (2011) 20–25.
[34] P. Nyamukamba, L. Tichagwa, C. Greyling, The influence of carbon doping on TiO_2 nanoparticle size, surface area, anatase to rutile phase transformation and photocatalytic activity, Mater. Sci. Forum, 712 (2012) 49–63.
[35] N. Wetchakun, B. Incessungvorn, K. Wetchakun, S. Phanichphant, Influence of calcination temperature on anatase to rutile phase transformation in TiO_2 nanoparticles synthesized by the modified sol–gel method, Mater. Lett., 82 (2012) 195–198.
[36] K.S.W. Sing, Reporting physisorption data for gas/solid systems with special reference to the determination of surface area and porosity, Pure Appl. Chem., 54 (1982) 2201–2218.
[37] J. Zhang, P. Zhou, J. Liuband, J. Yu, New understanding of the difference of photocatalytic activity among anatase, rutile and brookite TiO_2, Phys. Chem. Chem. Phys., 16 (2014) 20382–20386.
[38] Y. Su, J.S. Wu, X. Quan, S. Chen, Electrochemically assisted photocatalytic degradation of phenol using silicon-doped TiO_2 nanofilm electrode, Desalination, 252 (2010) 143–148.